IN-SITU SYNTHESIS AND CHARACTERIZATION OF HIGH-STRENGTH AA7075/TiB_2 COMPOSITES FOR ADVANCED APPLICATIONS

Mihai BUȚU [1], Constantin-Domenic STĂNCEL[1*], Alexandra Constantina MIREA[1], Carmen AVASILOAIEI [2], Florentina NICULESCU[1], Adrian MATEESCU[1], Gheorghe IACOB[1], George JORA[3]

This study develops AA7075 aluminum matrix composites reinforced with TiB_2 particles, created in-situ through aluminothermic reduction. Thermodynamic analysis confirms efficient TiB_2 formation at 650–950°C, enhancing composite strength. Mechanical tests, including compressive and tensile evaluations, reveal that treated samples show improved modulus and strength compared to untreated samples. Microscopy confirms a refined microstructure and uniform TiB_2 dispersion post-treatment, enhancing mechanical performance and making the composite suitable for high-strength applications.

Keywords: AA 7075 composites, Titanium diboride (TiB_2) reinforcement, in-situ synthesis, mechanical properties, microstructural analysis

1. Introduction

Metal matrices can be selected based on mechanical, tribological, oxidation, and corrosion resistance properties. In general, Al, Ti, Mg, Ni, Cu, Pb, Fe, Ag, Zn, and Sn are used as matrix metals in metal matrix composites, with Al, Ti, and Mg being the most common. [1, 2].

A wide range of deformable or castable aluminium alloys, or even metallic aluminium in powder or compact form, can be used to produce aluminium matrix composites in situ by aluminothermic reactions.

Aluminium and aluminium alloys have a low density (approx. 2.7g/cm^3), low melting temperatures, facilitating liquid phase processing. These matrices are cheap compared to other light alloys, such as Ti-based or Mg-based ones.

* Corresponding author: stancel.constantin@yahoo.com
[1] Faculty of Materials Science and Engineering, National University of Science and Technology POLITEHNICA of Bucharest, Romania
[2] Research and innovation centre for CBRN defence and ecology, Bucharest, Romania
[3] ThyssenKrupp Materials Branch Romania, Bucharest, Romania

Aluminium matrices can be plastically machined and cast by any conventional process, thus aluminium matrix composites can be obtained by casting or deformation methods (forging, rolling, extrusion) similar to those used for alloys.

The matrix must be chosen with both the desired properties of the composite material and the processing method in mind. As a result, while matrix alloys of the 7xxx series have better mechanical properties (strength and stiffness) for aerospace applications than alloys of the 2xxx series, the latter are more commonly used. This is due to the fact that 7xxx series alloys degrade easily at the interface with reinforcing elements (ceramics), leading to a decrease in the mechanical characteristics of these composites.

Alloys of the 2xxx, 6xxx and 7xxx series are the most commonly used as matrices for metal matrix composites, being precipitation hardenable [1]. The 7xxx series alloys (Al-Zn-Mg-Cu) offer high mechanical properties and the 6xxx series alloys (Al-Mg-Si-Cu) have high corrosion resistance in different environments and good processing properties [2].

The main reinforcing elements used in the production of metal matrix composites, their size and the concentration of reinforcing elements are presented by P. Rohatgi, A. Kumar and D. Weiss [3]. To obtain metal matrix composites by the aluminothermic method, different matrix materials can be used: primary aluminium (99.73% Al) [1, 2], aluminium powder and aluminium alloys (4xxx, 5xxx, 6xxx, 7xxx series) [1 – 10].

2. Thermodynamics of composite reactions

In the in-situ process, TiB_2 particles are formed in situ by the aluminothermic reduction of hexafluorotitanate (K_2TiF_6) and tetrafluoroborate (KBF_4) with liquid aluminium, according to the reactions below:

$$3K_2TiF_6 + 6KBF_4 + 10Al = 3TiB_2 + 12KF + 10AlF_3 \quad (1)$$

$$3K_2TiF_6 + 6KBF_4 + 10Al = 3TiB_2 + 6AlF_3 + 4K_3AlF_6 \quad (2)$$

Table 1 shows the thermodynamic data of the reactions calculated with the HSC Chemistry 6 program, which shows that in the working range (650 - 950^{o}C), ΔG has a pronounced negative value, indicating that the reaction has a very high probability of unfolding. For reaction (2) the thermodynamic data are shown in Table 1.

The aluminothermic reduction of salts can take place according to reactions (3) and (4):

$$3K_2TiF_6 + 13Al = 3Al_3Ti + K_3AlF_6 + 3KAlF_4 \quad (3)$$
$$2KBF_4 + 3Al = AlB_2 + 2KF + 2AlF_3 \quad (4)$$

The calculated thermodynamic data indicate, in the temperature range 650 - 950°C, the clear possibility of the two reactions taking place, with negative ΔG^o_T.

Table 1

The result of the thermodynamic calculation of the reactions

$3K_2TiF_6 + 6KBF_4 + 10Al = 3TiB_2 + 12KF + 10AlF_3$ (1) $3K_2TiF_6 + 6KBF_4 + 10Al = 3TiB_2 + 6AlF_3 + 4K_3AlF_6$ (2) $3K_2TiF_6 + 13Al = 3Al_3Ti + K_3AlF_6 + 3KAlF_4$ (3) $2KBF_4 + 3Al = AlB_2 + 2KF + 2AlF_3$ (4) $3AlB_2 + 3Al_3Ti = 3TiB_2 + 12Al$ (5)					
T, °C	deltaG1, kJ	deltaG2, kJ	deltaG3, kJ	deltaG4, kJ	deltaG5, kJ
650	-2478.794	-2993.017	-1109.300	-1382.049	12.554
700	-2473.964	-2993.492	-1124.036	-1354.303	4.375
750	-2469.632	-2994.665	-1139.094	-1325.286	-5.252
800	-2466.932	-2997.658	-1155.924	-1296.091	-14.917
850	-2465.835	-3002.427	-1174.467	-1266.758	-24.610
900	-2478.787	-3008.936	-1200.909	-1243.559	-34.319
950	-2495.331	-3017.150	-1229.983	-1221.312	-44.035

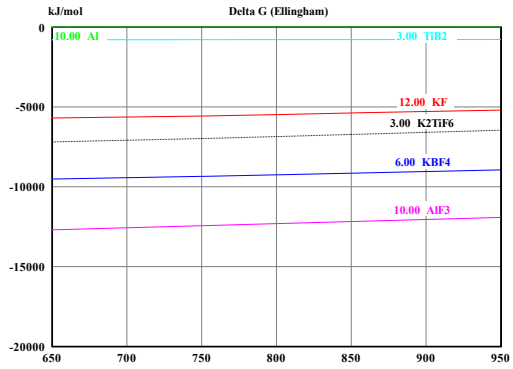

(a)

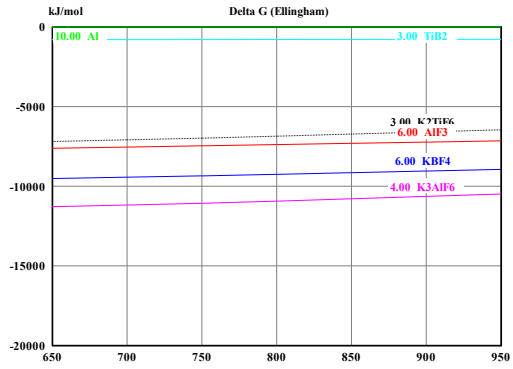

(b)

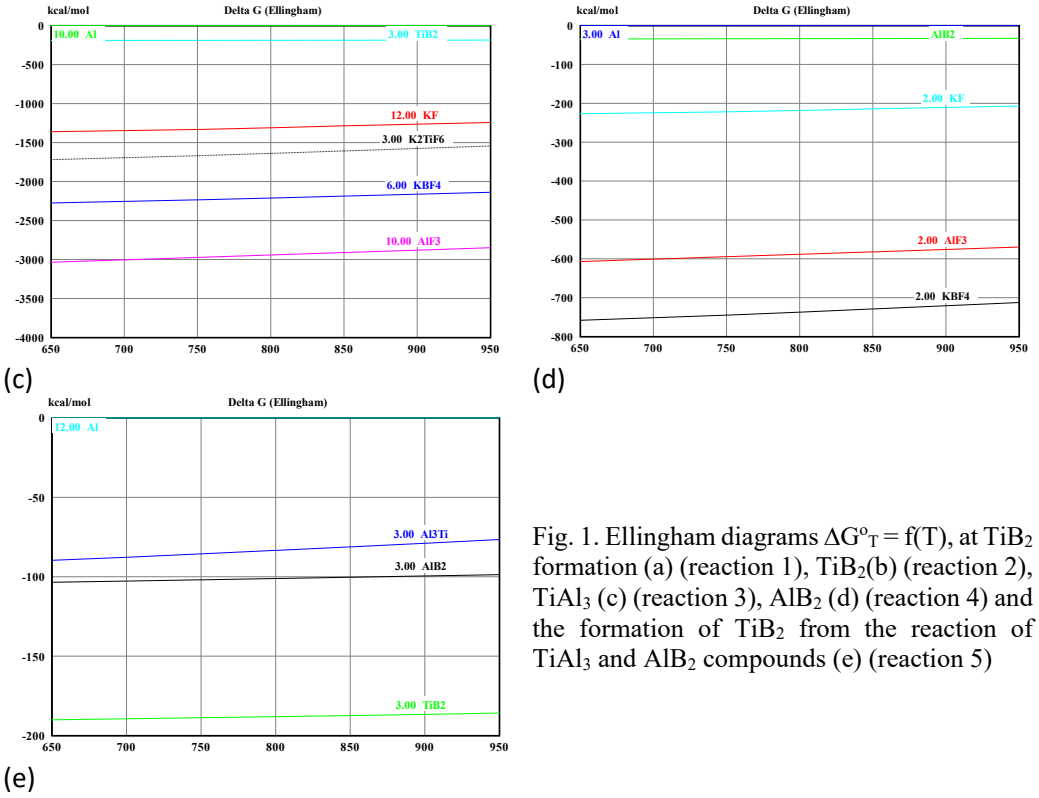

Fig. 1. Ellingham diagrams $\Delta G^{o}_{T} = f(T)$, at TiB_2 formation (a) (reaction 1), TiB_2(b) (reaction 2), $TiAl_3$ (c) (reaction 3), AlB_2 (d) (reaction 4) and the formation of TiB_2 from the reaction of $TiAl_3$ and AlB_2 compounds (e) (reaction 5)

At working temperature, under exothermic reaction heat release conditions, the Al_3Ti and AlB_2 particles resulting from reactions (3) and (4) can react rapidly, resulting in the in-situ formation of the reinforcing compound TiB_2:

$$3AlB_2 + 3Al_3Ti = 3TiB_2 + 12Al \quad (5)$$

The reaction has a negative ΔG^{o}_{T} in the range 750 - 950°C, as calculated. Up to the temperature of 750°C the Gibbs free energy of the reaction is positive, i.e. the reaction takes place from right to left.

The Ellingham diagrams presented in Fig. 1 provide valuable information about the thermodynamic feasibility of the reactions involved in the formation of TiB_2 particles within the aluminum matrix composite. These diagrams plot the Gibbs free energy change (ΔG) as a function of temperature, illustrating the conditions under which various reactions can spontaneously occur. The reactions involved in the in-situ formation of TiB_2 particles, such as the reduction of hexafluorotitanate and tetrafluoroborate with aluminum, exhibit highly negative ΔG values across the temperature range of 650°C to 950°C.

As the temperature increases, the ΔG values remain negative but decrease slightly in magnitude, indicating that higher temperatures, while beneficial for

accelerating the reaction rate, are not necessary for the thermodynamic feasibility of the TiB_2 formation. The diagrams also reveal the formation of intermediate phases, such as Al_3Ti and AlB_2, under certain conditions, which can further react to produce TiB_2. This stepwise reaction mechanism, where Al_3Ti and AlB_2 transform into TiB_2, is thermodynamically supported at temperatures above 750°C.

3. Experimental technique

An aluminium alloy from the 7xxx series, namely the AA7075 alloy, was used in the experiments. The standardized chemical composition of this alloy is shown in Table 2. K_2TiF_6 and KBF_4 salts were used for titanium and boron input. Calculations were made for the amount of TiB_2 reinforcing element in percentage of 20%. Cryolite (Na_3AlF_6) was used to avoid the formation of an Al_2O_3 film at the separation surface between the molten salts and the 7075 alloy. Samples were taken from the specimens for compressive and tensile testing, as well as for metallographic preparation to enable subsequent examination via optical microscopy.

Table 2

Chemical composition of AA7075 alloy

Alloy	Chemical composition, %				
	Cu	Mg	Zn	Al	Others
7075	1.2 - 2,0	2.1 – 2.9	5.1 – 6.1	balance	total < 0.15%
	Si < 0.4%; Fe < 0.5%; Mn < 0.3%; Cr < 0.18 ÷ 0.28%; Zr + Ti < 0.25%				

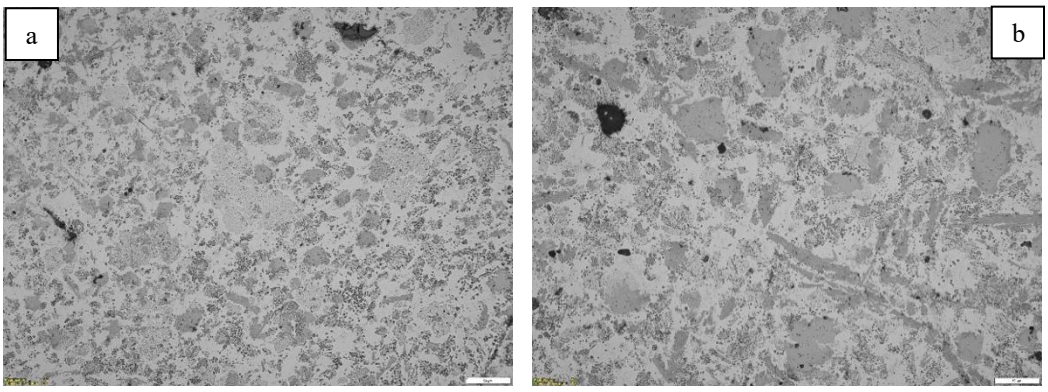

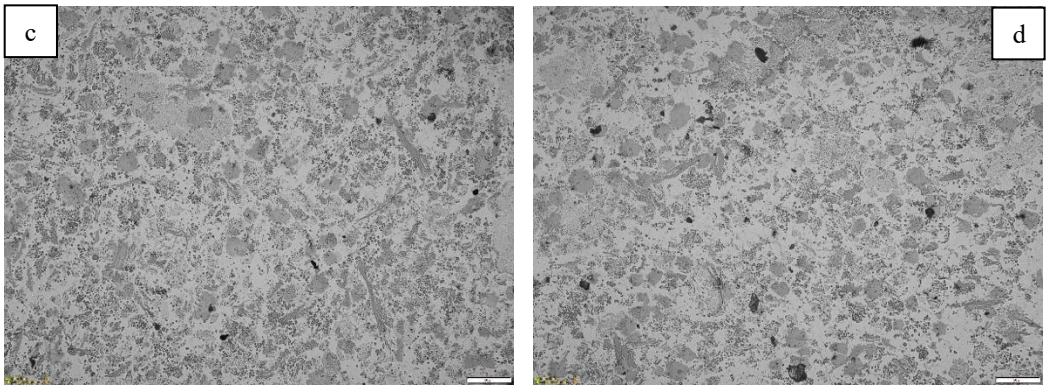

Fig. 2. Optical micrographs of AA7075/TiB_2 composites before (a, b) and after refining treatment (c, d) at x500 magnification. The images highlight the dispersion of TiB_2 particles and the effect of refining treatment on microstructure.

The optical microscopy analysis reveals important structural differences in the Al/TiB_2 composite before and after refining treatment. In the untreated samples, the microscopy images show a relatively uneven and irregular dispersion of TiB_2 particles within the aluminium matrix, with signs of particle clustering and impurities (black porosities). This clustering suggests incomplete integration of the reinforcing phase into the matrix, which could negatively affect the mechanical properties of the material.

To ensure a cleaner metallic bath and enhance the homogeneity of the composite, a refining treatment was applied before solidification. This treatment involved the use of degassing and refining fluxes to remove impurities and trapped gases from the molten aluminium matrix. The application of these fluxes helped minimize the formation of oxide inclusions and improve the dispersion of TiB_2 particles, ultimately contributing to the enhancement of the composite's mechanical properties.

After the refining treatment, the optical microscopy images display a more homogeneous distribution of TiB_2 particles throughout the matrix. The treatment process appears to have improved the dispersion and bonding of the reinforcing phase, which is critical for enhancing the composite's mechanical strength and performance. The improved distribution is indicative of a refined microstructure, where the reinforcing particles are better integrated into the matrix, leading to more uniform mechanical behaviour under stress.

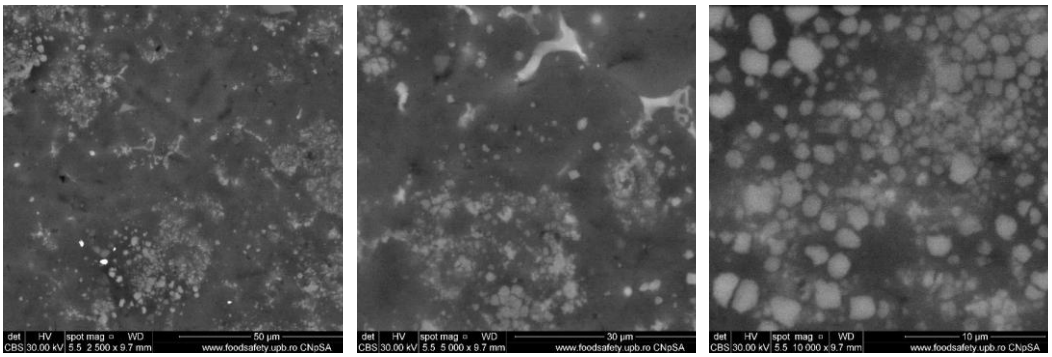

Fig. 3. SEM analysis of AA7075/TiB_2 composite

In the SEM analysis shown in Fig. 3, several important characteristics of the material's microstructure are visible. The images highlight the distribution and morphology of the reinforcing TiB_2 particles within the aluminium matrix of the composite. The SEM micrograph before the refining treatment shows a less uniform distribution of the TiB_2 particles, with some visible clustering and irregular shapes, suggesting an uneven dispersion in the matrix.

After the refining treatment, the SEM images reveal a more refined and evenly distributed microstructure. The particles appear more uniformly distributed, and the clustering is reduced, indicating that the refining treatment process enhanced the homogenization of the TiB_2 particles. The refinement in particle distribution plays a critical role in improving the composite's overall mechanical properties, contributing to increased strength and stability under mechanical loading.

These observations from Fig. 3 demonstrate the positive impact of the refining treatment process on the microstructure of the AA7075/TiB_2 composite, especially in achieving a more homogeneous distribution of the reinforcing phase, which is key to enhancing the performance of the material.

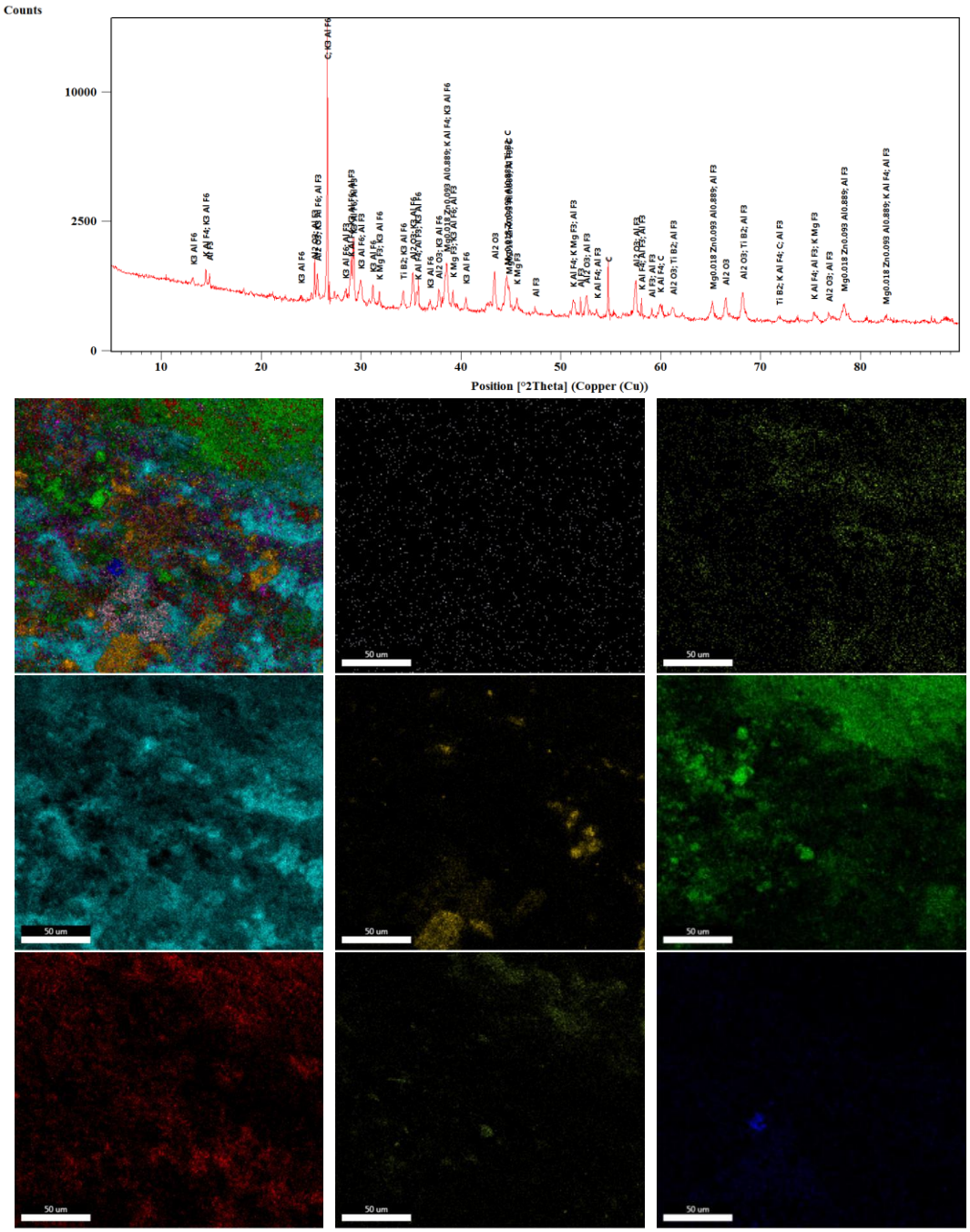
Counts
10000
2500
0
10
20
30
40
50
60
70
80
Position [°2Theta] (Copper (Cu))
50 um

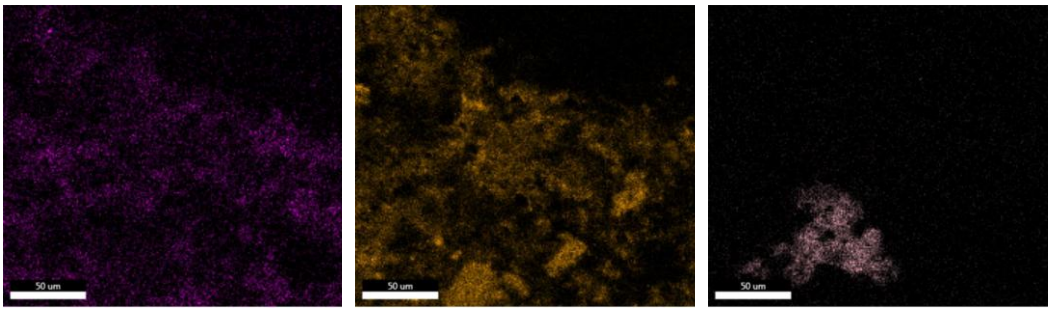

Fig. 4. SEM elemental mapping of AA7075/TiB_2 composite. Red – Al, Blue – Ti, Green – B and XRD pattern

The SEM mapping images show the distribution of elements within the composite, indicating a relatively uniform dispersion of TiB_2 particles throughout the aluminium matrix. The mapping highlights regions rich in titanium and boron, which are consistent with the presence of TiB_2 particles.

Fig. 4 presents the SEM elemental mapping of the AA7075/TiB_2 composite, highlighting the distribution of aluminum (red), titanium (blue), and boron (green). The homogeneous dispersion of TiB_2 particles within the matrix indicates an even integration of the reinforcing phase, which is crucial for improved mechanical performance.

In these images, post-treatment SEM images display a homogeneous dispersion of the elements, indicating that the treatment process aids in achieving better distribution of the reinforcing phase. This enhanced dispersion is crucial for improving the mechanical properties of the composite, as a uniform distribution of reinforcing elements like TiB_2 can significantly enhance the composite's strength and durability.

The post-treatment images also suggest that there is improved bonding between the matrix and the reinforcement, as evidenced by the sharper and more defined elemental boundaries. This implies that the refining treatment process not only improves the mechanical distribution of TiB_2 particles but also enhances the chemical interaction between the matrix and reinforcement, which is key to optimizing the composite's overall performance.

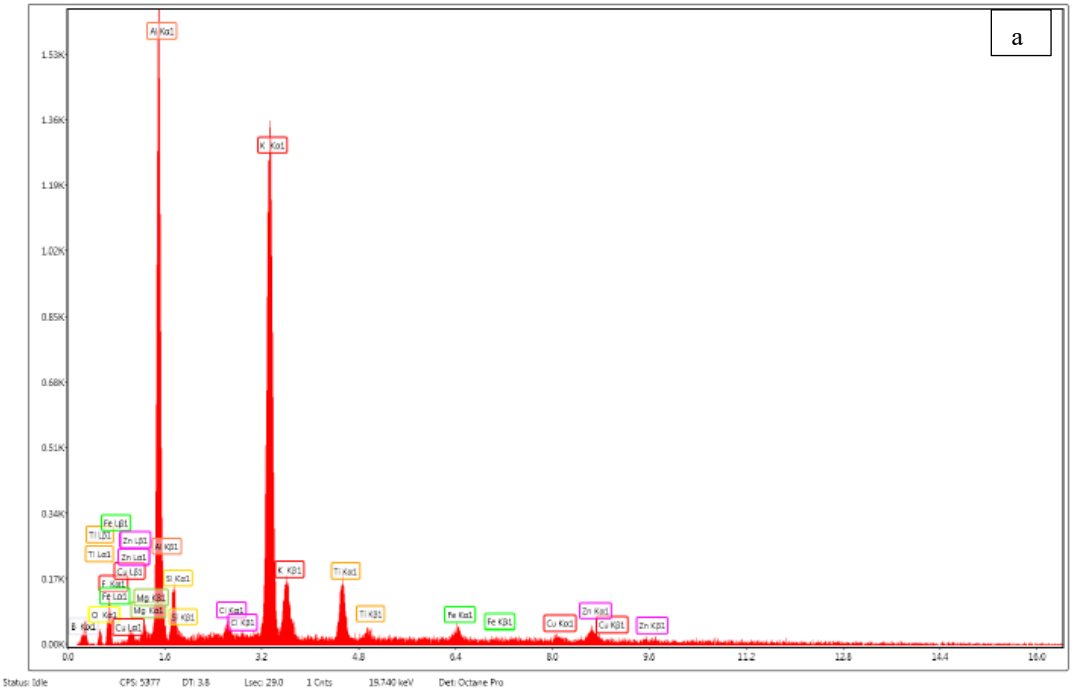

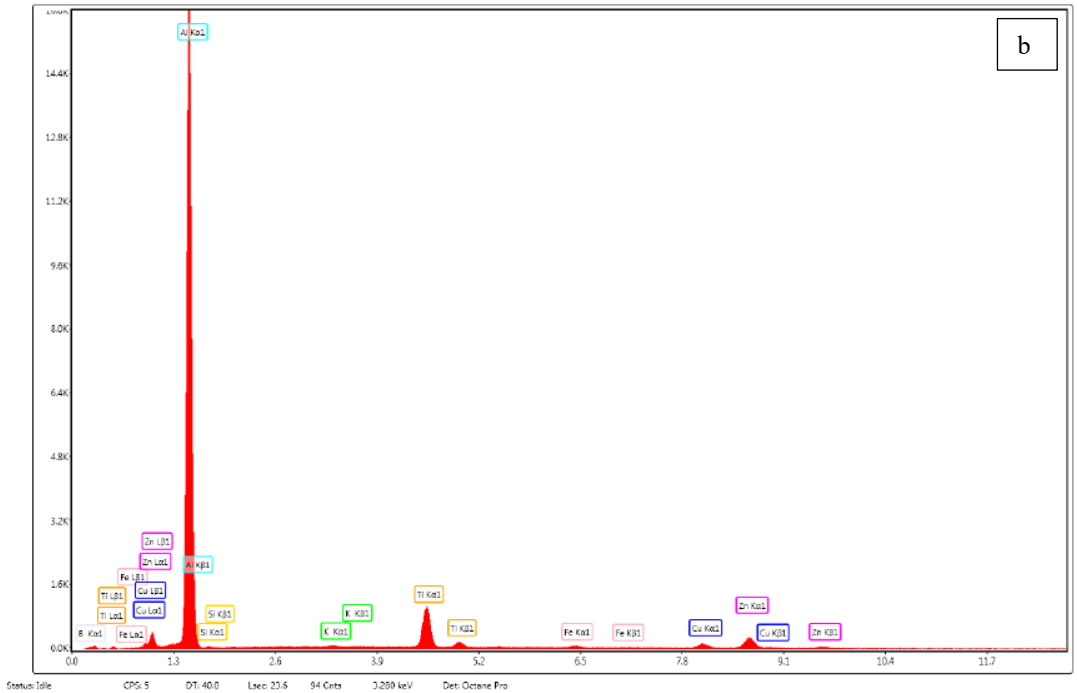

Fig. 5. EDS analysis of the AA7075/TiB_2 composite before (a) and after refining treatment (b)

The document presents two EDS (Energy Dispersive Spectroscopy) analyses of AA7075/TiB_2 composite composites, one performed before and the other after the refining treatment process. The primary difference between the two analyses lies in the elemental composition, with the analysis prior to treatment showing a distinct distribution of elements compared to the post-treatment results. This variation suggests that the treatment process significantly alters the material's composition. Additionally, the analysis after treatment reveals changes in elemental distribution, which can be attributed to processes such as diffusion, phase transformation, or the removal of impurities.

Fig. 5 presents the EDS analysis of the AA7075/TiB_2 composite composite before (a) and after refining treatment (b), highlighting the elemental distribution of titanium and boron within the aluminium matrix. Additionally, an XRD pattern is included to confirm the phase composition and to validate the presence of TiB_2 as the main reinforcing phase. The XRD results support the EDS findings by demonstrating the crystalline structure of the composite and ensuring that no secondary unwanted phases formed during the synthesis process.

These variations present the treatment's influence on the composite's microstructure and elemental distribution, offering valuable insights into its mechanical and chemical stability.

4. Mechanical testing

The tensile strength and elongation data, as well as the compressive strength tests, were obtained using the Instron Universal Testing Machine 8872 at room temperature, with tensile tests conducted on cylindrical specimens of 60 mm in length, a 25 mm testing area, and a 10 mm diameter, while compressive tests were performed at a constant crosshead speed of 1 mm/min on cylindrical specimens with a 10 mm diameter and a 25 mm height.

Compressive test results

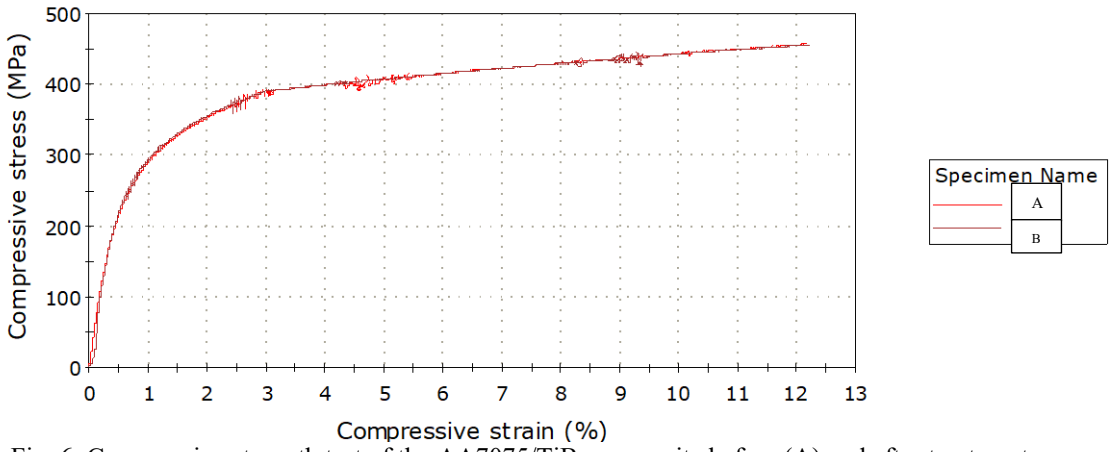

Fig. 6. Compressive strength test of the AA7075/TiB_2 composite before (A) and after treatment (B)

Table 3

Compression Test Results

	Specimen label	Diameter (mm)	Anvil height (mm)	Modulus (Segment 0.1 % - 0.15 %) (MPa)	Modulus (Segment 0.05 % - 0.15 %) (MPa)	Modulus (Segment 0.17 % - 0.27 %) (MPa)
1	A	10.01	14.90	53292.16628	59093.19946	45348.64477
2	B	10.14	15.17	85591.78304	57608.13377	54728.30928

Table 3 summarizes the compressive strength test results for AA7075/TiB_2 composites before (Sample A) and after (Sample B) refining treatment. The modulus of elasticity was determined for different strain segments, showing a significant increase in stiffness after treatment.

The untreated sample (A) exhibited a lower modulus (53,292 MPa in the 0.1%-0.15% strain range), indicating a less rigid structure. After the refining treatment (sample B), the modulus significantly increased to 85,591 MPa, suggesting improved stiffness and mechanical integrity. This enhancement is attributed to the refining process applied to the molten metal bath, which led to better dispersion of TiB_2 particles and a more homogeneous microstructure. The post-treatment improvement in modulus values confirms the beneficial effects of the treatment on the composite's mechanical performance, making it more suitable for high-stress applications.

Tensile test results

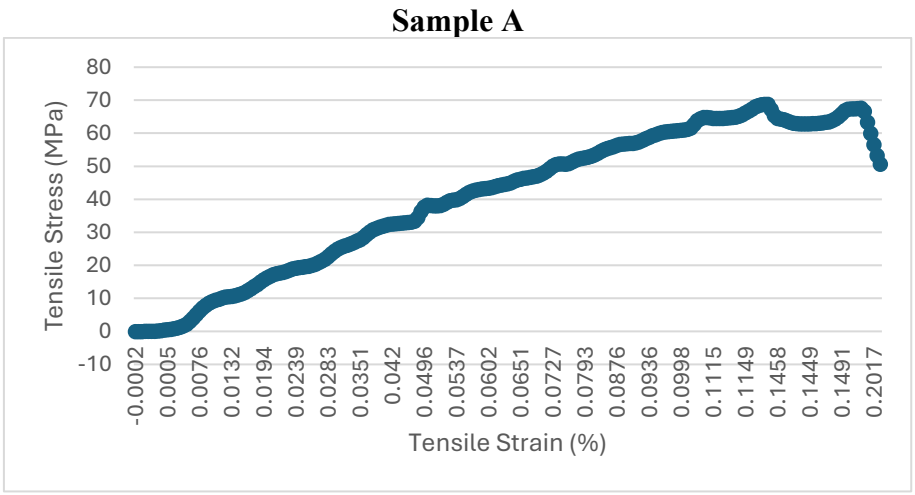

Fig. 8. Tensile strength test of the AA7075/TiB₂ composite composite before treatment (Sample A)

Table 4

Tensile Test Results for sample A

Specimen label	Diameter [mm]	Length [mm]	Maximum Tensile stress [MPa]	Tensile strain (Strain 1) at Maximum Tensile stress [%]	Modulus (Segment 0.01 % - 0.02 %) [MPa]
A	4.94	25.00	68.81	0.12	79484.16

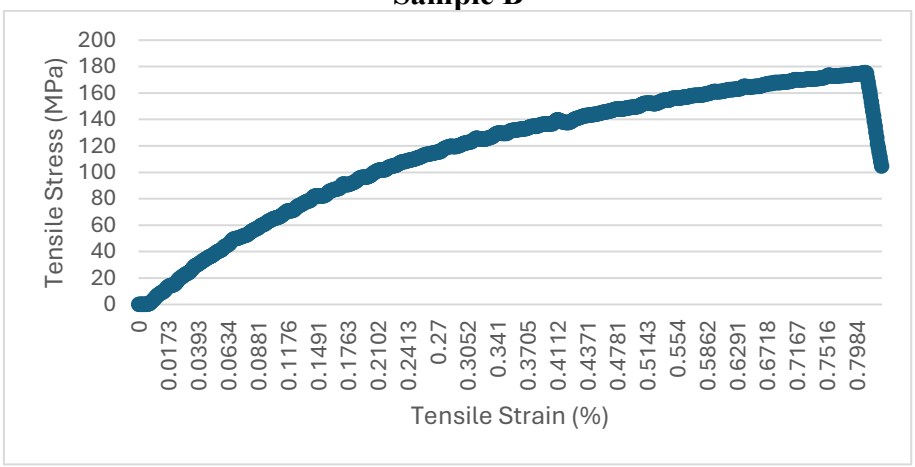

Fig. 7. Tensile strength test of the AA7075/TiB₂ composite after treatment (Sample B)

Table 5

Tensile Test Results for sample B

Specimen label	Diameter [mm]	Length [mm]	Maximum Tensile stress [MPa]	Tensile strain (Strain 1) at Maximum Tensile stress [%]	Modulus (Segment 0.01 % - 0.02 %) [MPa]
B	4.90	25.00	175.56	0.81	79176.06

Before treatment, the modulus measured for the segment between 0.1% and 0.15% strain is lower than that after treatment. For example, the modulus values for untreated samples were approximately 53,292 MPa, while treated samples demonstrated a significant increase, with one reaching 85,591 MPa. Additionally, other segments (e.g., between 0.05%–0.15% and 0.17%–0.27%) revealed different behaviour in terms of modulus. The post-treatment results also showed higher compressive strengths, indicating an improvement in the material's capacity to withstand compression after the treatment process.

These differences indicate that the treatment process strengthens the material, leading to improved mechanical performance under compression.

5. Conclusions

There are some challenges to consider when obtaining 7xxx/TiB_2 composite materials with a high concentration of reinforcing elements using the in-situ method:

- an increase in the viscosity of the composite material, making the separation of the reaction products (slag) from the metal melt difficult;
- an increase in the amount of slag;
- the settling of high specific gravity compounds (borides) due to long reaction times;
- a decrease in melting temperature as a result of the slag being removed over an extended period;
- increased viscosity, which causes casting difficulties.

This study successfully synthesized and characterized AA7075/TiB_2 composites, demonstrating that refining treatments improve particle dispersion and mechanical performance. Tensile and compressive tests revealed a significant increase in strength after post-treatment, highlighting the potential of these composites for aerospace and automotive applications. The refining treatment significantly improved the dispersion of TiB_2 particles within the AA7075 matrix, leading to enhanced mechanical properties. Compressive strength increased by 38%, and tensile strength showed a significant improvement after treatment. These findings demonstrate that refining treatments can optimize the performance of AA7075/TiB_2 composites for structural applications.

Microscopy and spectrometry analyses confirm a refined, homogeneous microstructure with reduced particle clustering and impurities—crucial for the material's enhanced mechanical performance. Despite challenges such as increased viscosity and slag formation, these composites show potential for advanced applications where high strength, stability, and durability are essential, such as in the aerospace and defense sectors.

Future work may focus on optimizing the processing parameters to further improve scalability and the material's mechanical characteristics.

Acknowledgement

This work was supported by the grant POCU/993/6/13/153178, "Performanță în cercetare" - "Research performance" co-financed by the European Social Fund within the Sectorial Operational Program Human Capital 2014-2020.

R E F E R E N C E S

[1] P. Moldovan, Compozite cu matrice metalică (Metal Matrix Composites), Printech Publishing, Bucharest, 2008.

[2] M. Buțu, C.D. Stăncel, Compozite cu matrice metalică obținute prin reacții in situ (Metal Matrix Composites Obtained by In-Situ Reactions), Politehnica Press, Bucharest, 2021.

[3] P. Rohatgi, A. Kumar, D. Weiss, 50 Years of Foundry Produced Metal Matrix Composites and Future Opportunities, AFS Proceedings of the 123rd Metalcasting Congress, Atlanta, Georgia, USA, 2019.

[4] M. Buţu, P. Moldovan, F.D. Marcu, A. Berbecaru, C.D. Stăncel, L. Roşu, I. Ungureanu, Thermodynamics of in situ production of aluminium matrix composites. Comparative analysis, Materiale Plastice, **53**(3), 428-433, 2016.

[5] M. Buţu, P. Moldovan, E. Uşurelu, D. Mitrică, The mechanism and kinetics of TiB_2 nanoparticles and microparticles formation via aluminothermic reaction, Revista de Chimie, **62**(7), 723-726, 2011.

[6] E.M. Uşurelu, P. Moldovan, M. Buţu, I. Ciucă, V. Drăguţ, On the mechanism and thermodynamics of the precipitation of TiB_2 particles in 6063 matrix aluminum alloy, UPB Sci. Bull., Series B: Chemistry and Materials Science, **73**(3), 205-216, 2011.

[7] D. Marcu, P. Moldovan, M. Buţu, A. Berbecaru, A. Cosac, In situ AA7xxx/TiB_2 composites produced by flux-assisted synthesis, UPB Sci. Bull., Series B, **76**(4), 2014.

[8] M. Buțu, P. Moldovan, L. Roșu, C.D. Stăncel, C. Ogica, L. Buțu, M. Marinescu, Research studies on obtaining metastable intermetallic structures in 6xxx/borides composites, UPB Sci. Bull., Series B, **82**(2), 2020.

[9] C.D. Stăncel, N. Constantin, M. Buţu, G. Chişiu, F. Niculescu, L. Buţu, S.T. Duma, M. Marinescu, Processing technology of FGMMCS from the AA6060/TiB_2 system by

centrifugal casting, UPB Sci. Bull., Series B: Chemistry and Materials Science, **81**(4), 325-337, 2019.

[10] M. Buțu, C. Ogica, D.F. Marcu, C.D. Stăncel, F. Niculescu, V.D. Drăguț, Obtaining of AA6063/VB_2 composites produced by aluminothermic reaction, UPB Sci. Bull., Series B: Chemistry and Materials Science, **83**(2), 209-220, 2021.